Ecosystem carbon storage capacity as affected by disturbance regimes: A general theoretical model

Ensheng Weng,[1] Yiqi Luo,[1] Weile Wang,[2] Han Wang,[3] Daniel J. Hayes,[4] A. David McGuire,[5] Alan Hastings,[6] and David S. Schimel[7]

Received 28 March 2012; revised 8 June 2012; accepted 9 June 2012; published 27 July 2012.

[1] Disturbances have been recognized as a key factor shaping terrestrial ecosystem states and dynamics. A general model that quantitatively describes the relationship between carbon storage and disturbance regime is critical for better understanding large scale terrestrial ecosystem carbon dynamics. We developed a model (REGIME) to quantify ecosystem carbon storage capacities ($E[x]$) under varying disturbance regimes with an analytical solution $E[x] = U \cdot \tau_E \cdot \frac{\lambda}{\lambda + s\tau_1}$, where U is ecosystem carbon influx, τ_E is ecosystem carbon residence time, and τ_1 is the residence time of the carbon pool affected by disturbances (biomass pool in this study). The disturbance regime is characterized by the mean disturbance interval (λ) and the mean disturbance severity (s). It is a Michaelis-Menten-type equation illustrating the saturation of carbon content with mean disturbance interval. This model analytically integrates the deterministic ecosystem carbon processes with stochastic disturbance events to reveal a general pattern of terrestrial carbon dynamics at large scales. The model allows us to get a sense of the sensitivity of ecosystems to future environmental changes just by a few calculations. According to the REGIME model, for example, approximately 1.8 Pg C will be lost in the high-latitude regions of North America (>45°N) if fire disturbance intensity increases around 5.7 time the current intensity to the end of the twenty-first century, which will require around 12% increases in net primary productivity (NPP) to maintain stable carbon stocks. If the residence time decreased 10% at the same time additional 12.5% increases in NPP are required to keep current C stocks. The REGIME model also lays the foundation for analytically modeling the interactions between deterministic biogeochemical processes and stochastic disturbance events.

Citation: Weng, E., Y. Luo, W. Wang, H. Wang, D. J. Hayes, A. D. McGuire, A. Hastings, and D. S. Schimel (2012), Ecosystem carbon storage capacity as affected by disturbance regimes: A general theoretical model, *J. Geophys. Res.*, *117*, G03014, doi:10.1029/2012JG002040.

1. Introduction

[2] Disturbances can profoundly affect ecosystem carbon (C) storage and dynamics by generating spatially heterogeneous landscapes, reducing ecosystem production, depleting one or more C pools, and relocating C distribution among these pools [*Goetz et al.*, 2007; *Turner*, 2010]. Climate warming and human activities are increasing the frequencies, severities, and spatial coverage of disturbances, such as fires [*Bowman et al.*, 2009; *Turetsky et al.*, 2011], storms [*Emanuel*, 2005; *Webster et al.*, 2005], and insect outbreaks [*Kurz et al.*, 2008c]. Improving understanding of the impacts of disturbances on ecosystem C is required for accurately estimating the feedbacks between C cycle and climate change [*Kurz et al.*, 2008b; *Luo and Weng*, 2011; *Running*, 2008].

[3] The impacts of individual disturbance events on ecosystem carbon processes have been extensively studied. For example, the effects of fire on landscape heterogeneity [*Turner et al.*, 1994], C and nitrogen dynamics [*Kashian et al.*, 2006; *Smithwick et al.*, 2009], and C storage recovery patterns [*Kashian et al.*, 2005; *Kashian et al.*, 2006] have been systematically investigated following the 1988 Yellowstone Fires. Modeling studies have been conducted to identify the key mechanisms of disturbance events influencing C processes and explore possible responses of C dynamics to changes in disturbance regimes induced by climate warming. By modeling analysis with the Biome-Biogeochemical Cycle

[1]Department of Botany and Microbiology, University of Oklahoma, Norman, Oklahoma, USA.
[2]NASA Ames Research Center, Moffett Field, California, USA.
[3]School of Electrical and Computer Engineering, University of Oklahoma, Norman, Oklahoma, USA.
[4]Environmental Sciences Division, Oak Ridge National Laboratory, Oak Ridge, Tennessee, USA.
[5]U.S. Geological Survey, Alaska Cooperative Fish and Wildlife Research Unit, University of Alaska, Fairbanks, Fairbanks, Alaska, USA.
[6]Department of Environmental Science and Policy, University of California, Davis, California, USA.
[7]NEON Inc., Boulder, Colorado, USA.

Corresponding author: E. Weng, Department of Botany and Microbiology, University of Oklahoma, Norman, OK 73019, USA. (wengensheng@gmail.com)

0148-0227/12/2012JG002040

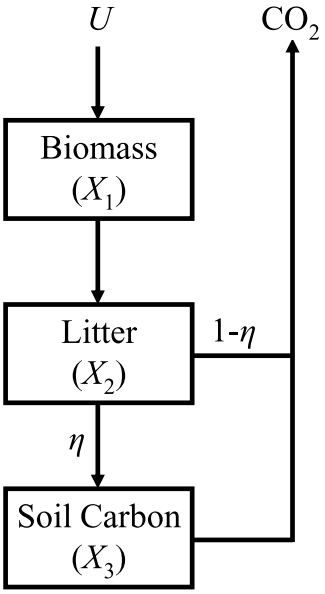

Figure 1. Ecosystem C cycle model (conceptual biogeochemical cycle model). U is the ecosystem carbon input (net primary production (NPP)). The model has three carbon pools: biomass (X_1), litter (X_2), and soil organic matter (SOM) (X_3). η is the fraction of carbon transferred to the SOM pool from the litter pool.

model, *Bond-Lamberty et al.* [2007] found that disturbance events were the dominant driver of boreal forest carbon balance in the central Canada. *Kurz et al.* [2008c] proposed that insect outbreaks in the boreal forests in Canada may transform those forests from C sinks to sources due to the substantial reductions of gross primary production (GPP) according the modeling results of CBM-CFS3. *Balshi et al.* [2009, 2007] analyzed the effects of historical fires on current C dynamics of the high-latitude regions of North America and suggested that fires could substantially increase the vulnerability of the C storage in the boreal forests within the twenty-first century.

[4] The effects of individual disturbance events can be easily misinterpreted and substantially overestimated without considering the long-term dynamics of disturbance regimes. Terrestrial ecosystems can rapidly recover from individual disturbance events [*Romme et al.*, 2011; *Turner*, 2010], making them carbon neutral from a long-term view [*Kashian et al.*, 2006]. Similarly over a large special scale, the carbon losses triggered by a disturbance event in one area can be fully compensated by the recovery in other areas if the regional disturbance regime does not change [*Stinson et al.*, 2011]. Changes in disturbance regimes, which are usually characterized by disturbance frequencies and severities, can have more profound impacts on ecosystem C storage and dynamics. For example, suppression of fires leads to increases in carbon stocks in Minnesota oak savanna [*Tilman et al.*, 2000], while increases in fire frequencies during 1980s and fire severity in recent decades reduced Canadian forest biomass [*Kurz and Apps*, 1999; *Stinson et al.*, 2011]. The biomass of a savanna ecosystem nonlinearly decreases with fire severity and increases with fire return intervals according to a 50-year fire experiment in Africa [*Ryan and Williams*, 2011]. Thus, it's necessary to explore how disturbance regimes affect C dynamics at large spatial scales.

[5] Ensemble simulations with varied disturbance regimes are conducted to explore the general patterns of ecosystem C dynamics with different disturbance regimes. For example, *Smithwick et al.* [2007] showed the patterns of C storage with changes in disturbance frequencies and severities. *Kurz et al.* [2008a] explored to what extent the increases in net primary productivity (NPP) can compensate the carbon losses induced by increased fire frequency. *Metsaranta et al.* [2010] explored the implications of future disturbance regimes on the carbon balance of Canada's managed forests. These ensemble simulations greatly improved our understanding of ecosystem C dynamics at changing disturbance regimes. However, the computationally intensive ensemble simulations can only explore some possibilities of multi-factorial changes and are usually intractable. It is critical to develop a holistic system that integrates the deterministic C processes and stochastic disturbance regimes for improving our predictive understanding of ecosystem C dynamics at large scales.

[6] In this study, we developed a model to analytically describe ecosystem C storage as a function of ecosystem internal processes and disturbance regimes based on explicit mathematical descriptions of the recovery patterns of ecosystem C content and the probability density distributions of disturbances. We named the model REGIME to emphasize changes to disturbance regimes as a control over biogeochemical C processes. The REGIME model was tested against the simulations of a well established terrestrial biosphere model, the Terrestrial Ecosystem Model (TEM) [*Hayes et al.*, 2011; *McGuire et al.*, 2010] in the high-latitude regions of North America (>45°N). This model provides a framework for extrapolating the observations of ecosystem carbon dynamics at site scales to large spatial scales with information of disturbances and a tool of representing ecosystem states and processes for terrestrial C cycle modeling studies. It also allows us to estimate large scale ecosystem carbon storage dynamics just by a few calculations. We illustrated these application perspectives by examples in discussion.

2. Methods

[7] We adopt a three-pool model (Figure 1) to represent the ecosystem C processes, and a probabilistic description of disturbance frequency and severity to represent disturbance regimes. We treat disturbances as Poisson events in mathematical derivation and examine the sensitivities to alternative descriptions of the system through simulations. The details of the model and the assumptions about disturbance regimes and their impacts on ecosystem C processes are described below.

2.1. Ecosystem C Cycle Model

[8] We used a conceptual biogeochemical cycle (BGC) model to describe ecosystem C cycles in biomass (X_1), litter (X_2), and soil organic matter (SOM) (X_3) carbon pools (Figure 1). For an ecosystem developed from bare ground, the model can be described by equation (1).

$$\begin{aligned} &\frac{dX(t)}{dt} = AR^{-1}X(t) + BU(t) \\ &X(0) = (\,0 \quad 0 \quad 0\,)', \end{aligned} \tag{1}$$

Table 1. Model Parameters

Parameter	*Definition*	*Model*
A	Carbon transfer matrix	Conceptual BGC
B	Allocation vector of net primary production	Conceptual BGC
X_1	Biomass carbon pool (Kg C m^{-2})	Conceptual BGC
X_2	Litter carbon pool (Kg C m^{-2})	Conceptual BGC
X_3	Soil organic matter (SOM) carbon pool (Kg C m^{-2})	Conceptual BGC
$X(t)$	Vector for carbon pools at time t	Conceptual BGC
U_0	Reference NPP (Kg C m^{-2} yr^{-1})	Conceptual BGC
$U(t)$	NPP at time t (Kg C m^{-2} yr^{-1})	Conceptual BGC
x	Ecosystem total carbon (Kg C m^{-2})	REGIME
τ_1	Carbon residence time of biomass (yrs)	Conceptual BGC/REGIME
τ_2	Carbon residence time of litter (yrs)	Conceptual BGC/REGIME
τ_3	Carbon residence time of SOM (yrs)	Conceptual BGC/REGIME
τ_E	Ecosystem carbon residence time (yrs)	Conceptual BGC/REGIME
R	Diagonal matrix for carbon residence times	Conceptual BGC
η	The ratio of carbon transferred to SOM from litter pool	Conceptual BGC/REGIME
r	A random variable representing the occurrence of large-disturbances (1 for the occurrence, 0 for null)	Conceptual BGC
s	The fraction of biomass removed by a disturbance event (0–1)	Conceptual BGC/REGIME
λ	The mean disturbance interval (yrs)	REGIME/Disturbance regime
σ	Disturbance index (s/λ) (Kg C Kg C^{-1} yr^{-1})	REGIME
Ξ	Disturbance carbon transfer matrix	Conceptual BGC

where $X(t)$ is ecosystem carbon content at time t; A is a 3×3 matrix representing carbon transfer among the three pools. Here, $A = \begin{pmatrix} -1 & 0 & 0 \\ 1 & -1 & 0 \\ 0 & \eta & -1 \end{pmatrix}$ and η is carbon transfer coefficient from the litter pool to the SOM pool. R is a 3×3 diagonal matrix. The diagonal elements, τ_1, τ_2, and τ_3, are the residence times of the carbon in biomass, litter, and SOM, respectively. B is a vector of allocation coefficients of carbon influx (i.e., net primary production, NPP) to the three pools, $B = (1 \quad 0 \quad 0)'$. $U(t)$ is the carbon influx, i.e., NPP, at time t (see Table 1 for notations). This type of C-cycle model formulation has been widely used in ecosystem C-cycle modeling, such as in CENTURY model [*Parton et al.*, 1993], CASA [*Potter and Klooster*, 1997], and TECO [*Luo et al.*, 2003; *Weng and Luo*, 2011].

2.2. Disturbance Regime

[9] Characterizing disturbance regimes by their frequencies and severities has been employed frequently, such as in *Turner et al.* [1993] and *Smithwick et al.* [2007] who explored ecosystem states and C dynamics with effects of disturbances, respectively. Here, the disturbance regime is described by its mean disturbance interval and severity, and their probability density functions (PDFs). The ecosystem carbon dynamics that are affected by disturbances are described by the following equation:

$$\frac{dX(t)}{dt} = AR^{-1}X(t) + BU(t) + r \cdot s \cdot \Xi X(t), \tag{2}$$

where r is a discrete random variable, taking the value either 0 or 1 ($r \in \{0, 1\}$). It is used to indicate the occurrence of a disturbance event. The probability of a disturbance event happened in a given year is defined as $P(r = 1) = 1/\lambda$. As a result of this definition, the disturbance events are assumed to be Poisson events and therefore the interval between two consequential disturbance events is an exponential distribution. λ is the point mean disturbance interval, the time that a point in the region will experience a disturbance event on average, which contains the information of disturbance return intervals and the area affected by disturbance events, i.e., disturbance size [*Baker*, 2009; *Baker and Ehle*, 2001]. s is disturbance severity, defined as the fraction of biomass removed by a disturbance event, ranging from 0 to 1. The matrix Ξ represents carbon losses and transfer among the three carbon pools induced by a disturbance event. According to our assumptions in this study, the disturbance carbon transfer matrix (Ξ) is $\begin{pmatrix} -1 & 0 & 0 \\ 0 & 0 & 0 \\ 0 & 0 & 0 \end{pmatrix}$. In numerical simulations conducted in this study, assuming NPP (U) of 1.2 Kg C $m^{-2} \cdot yr^{-1}$, τ_1 20 yrs, τ_2 5 yrs, τ_3 60 yrs, and η 0.25 provides a reasonable system, which is close to a temperate forest [*Hamilton et al.*, 2002]. Given these parameter values, the ecosystem carbon residence time, τ_E, is 40 yrs ($\tau_E = \tau_1 + \tau_2 + \tau_3 \cdot \eta = 40$ yrs).

2.3. Sensitivity Tests

[10] Different assumptions on disturbance recurrence frequency and ecosystem recovery pattern could have a significant impact on the predictions of ecosystem C pools. We tested the assumptions of recovery patterns of NPP and PDFs of disturbance return intervals, i.e., the dependency of disturbance on ecosystem state, by model simulations.

[11] Forest NPP usually decreases sharply at a disturbance event (e.g., fire) and then recovers gradually. After approaching the peak level, it may decline slightly before stabilized [*Gower et al.*, 1996; *Ryan et al.*, 1997]. We conducted model simulations to test the biases induced by the assumption of constant NPP over time in the approximation of large spatial scale ecosystem carbon storage under influences of disturbances. The realistic NPP pattern was generated by the following equations:

$$\begin{aligned} GPP(t) &= GPP_{\max} \cdot \left(1 - e^{-[X_1(t)/L + a]}\right) \\ U(t) &= (1 - b) \cdot GPP(t) - f \cdot X_1(t), \end{aligned} \tag{3}$$

where, GPP_{max} is the maximum GPP, 2.4 Kg C $m^{-2} \cdot yr^{-1}$ in this study. L is an empirical coefficient; a is a constant used to allow initial NPP when biomass (X_1) is zero. We used 2.4 and 0.2 for L and a, respectively, and constants b and f are 0.3 and 0.02, respectively.

[12] Both Weibull and exponential distributions are widely used to describe disturbance intervals [*Clark*, 1990; *Johnson and Gutsell*, 1994; *Katz et al.*, 2005; *Van Wagner*, 1978]. The Weibull distribution is usually used in the disturbances that are related to the states of ecosystems (e.g., fire) for its flexibility to represent the changes in the disturbance occurrence probability over time by varying its shape factor [*Grissino-Mayer*, 1999].

$$f(T;\lambda,k) = \begin{cases} \frac{k}{\lambda}\left(\frac{T}{\lambda}\right)^{k-1} e^{-(T/\lambda)^k} (T \geq 0) \\ 0 \qquad\qquad\qquad\quad (T < 0) \end{cases}, \tag{4}$$

where k is the shape factor. The exponential distribution is a special case of the Weibull distribution with $k = 1$. In our ecosystem C simulations, the disturbance severity s was assumed equal to 1 and the disturbance intervals were sampled from the Weibull distributions with the shape factor (k) varying from 1.0 (an exponential distribution) to 2.0 (a typical value for fires) [*Baker*, 1989; *Grissino-Mayer*, 1999]. The mean carbon content for each combination of the mean disturbance interval and the shape factor of Weibull distribution k was the average over 65000 modeled grids after an 800 years' model run.

2.4. Comparison With the Simulations of the TEM Model

[13] We compared the predictions of the REGIME model with the simulations of a well established biogeochemical model, the Terrestrial Ecosystem Model (TEM). The TEM is a process-based ecosystem model that describes carbon and nitrogen dynamics of plants and soils for terrestrial ecosystems of the globe [*McGuire et al.*, 2010]. It was first published 20 years ago [*Raich et al.*, 1991] and since then has been applied in numerous studies on terrestrial ecosystem responses to global warming, changes in atmospheric CO_2 concentration [*VEMAP Members*, 1995], land use change [*McGuire et al.*, 2001], and disturbances [*Balshi et al.*, 2007].

[14] Here we used its latest version developed by *Hayes et al.* [2011] and *McGuire et al.* [2010]. The model was equilibrated with a 900-year model run using the climatic data of the year 1901, and then the simulations from 1901 to 2006 were driven by the actual observations of climatic variables (e.g., precipitation and air temperature) from the Climate Research Unit (1901–2002) [*Mitchell and Jones*, 2005] and NCEP/NCAR Reanalysis 1 data sets (2002–2006) [*Drobot et al.*, 2006], atmospheric CO_2 concentration [*Keeling and Whorf*, 2005], and disturbance events including fires and harvests [*Balshi et al.*, 2007]. (For more details, see *Hayes et al.* [2011].) The simulated yearly vegetation C content, NPP, litter fall, harvest and disturbance-induced carbon losses in the high-latitude regions (latitudes >45°N) of North America were used in this analysis.

[15] The whole region in our study was divided into 24 subregions according to the provincial or state boundaries. Regional averaged NPP (U), litter fall (L), heterotrophic respiration (RH), vegetation and soil C content (C_{veg}, C_{soil}), fire-induced C loss ($C_{fire,veg}$, $C_{fire,soil}$), and harvest ($C_{harvest}$) were calculated by averaging the values at each simulation grid (0.5° × 0.5°) for the recent 30 years (1977–2006). Vegetation C residence time (τ_{veg}) was calculated by current vegetation C content divided by annual litter fall, the output from the vegetation C pool. Potential vegetation C content is calculated by $U \times \tau_{veg}$. Soil C residence time (τ_{soil}) was calculated by current soil C content divided by annual heterotrophic respiration (C_{soil}/RH). The potential soil C content ($C_{soil,potential}$) was calculated by $U \times \tau_{soil}$.

[16] For comparing with the simulated disturbance effects, we defined a disturbance index ($\sigma = s/\lambda$), which combined disturbance severity and frequency. The disturbance intensity index for each simulation year in the TEM was calculated by $(C_{fire} + C_{harvest})/C_{pool}$, which was equivalent to s/λ in the REGIME model. C_{pool} is C_{veg} or C_{soil}, depending on which pool is the target. The soil C content with impacts of disturbances was calculated by the following equation:

$$C_{soil,cal} = U \cdot \tau_{soil} \cdot \frac{1}{1 + \sigma_{veg} \cdot \tau_{veg}} \cdot \frac{1}{1 + \sigma_{soil} \cdot \tau_{soil}}, \tag{5}$$

where σ_{veg} and σ_{soil} are the disturbance intensity for vegetation and soil, respectively. This equation considers the effects of disturbances (fires and harvests) on the vegetation pool (σ_{veg}) and the soil carbon pool (σ_{soil}).

3. Results

3.1. Analytical Solution: The REGIME Model

[17] As described in the methods, we treat the disturbances as a Poisson process in depth with our mathematical approach, where the disturbance intervals follow an exponential distribution (equation (6)).

$$f(T;\lambda) = \begin{cases} \frac{1}{\lambda} \cdot e^{-\frac{1}{\lambda}T}, T \geq 0 \\ 0 \qquad\quad , T < 0 \end{cases}, \tag{6}$$

where T is the interval between two consecutive disturbance events and λ is the mean disturbance interval according to the properties of the exponential distribution.

[18] With the assumption that the carbon influx (NPP) and residence are not affected by disturbances, the recovery pattern of biomass is:

$$X_1 = U\tau_1\left(1 - e^{-t/\tau_1}\right) + x_{1,0} \cdot e^{-t/\tau_1}, \tag{7}$$

where X_1 is carbon content of the biomass pool, $x_{1,0}$ is the legacy carbon of the biomass pool remaining after a disturbance event, U is carbon influx, τ_1 is carbon residence time of the biomass pool, and t is the time since last disturbance event. Equation (7) is the solution of the differential equation describing carbon accumulation at a constant input rate U and decay at rate ($1/\tau_1$) (equation (1)). The first term of the right side [$U\tau_1(1 - e^{-t/\tau_1})$] represents the accumulation of new carbon and the second term ($x_{1,0} \cdot e^{-t/\tau_1}$) is the decay of legacy carbon.

[19] Integration of the exponential distribution of disturbance intervals (equation (6)) with the ecosystem carbon

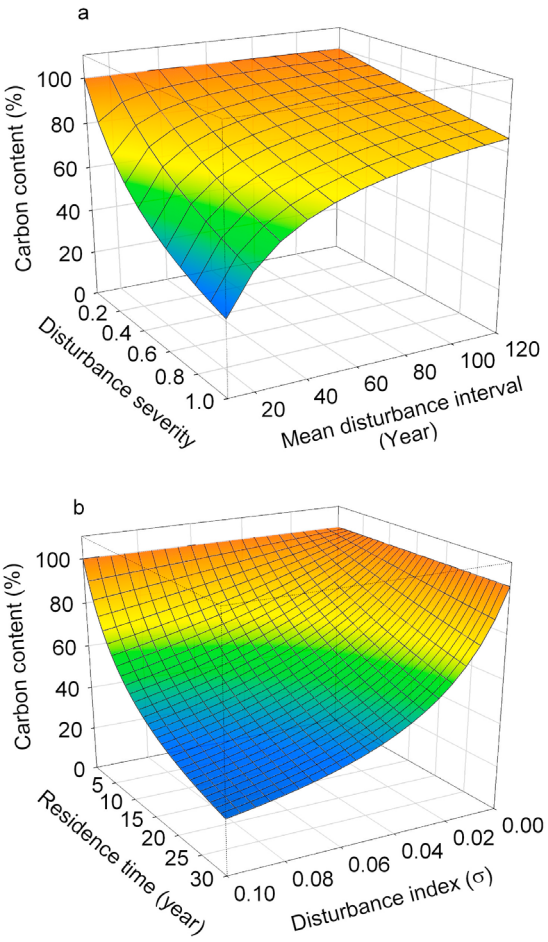

Figure 2. Ecosystem carbon contents (percentage of potential, $U\tau_E$) with (a) changes in mean disturbance interval and severity, and (b) changes in residence time and disturbance index (σ = s/λ) based on equation (9).

recovery curve (equation (7)) at a given disturbance severity, s, yields the expectation of biomass, $E[X_1]$:

$$E[X_1] = U \cdot \tau_1 \cdot \frac{\lambda}{\lambda + s\tau_1}. \quad (8)$$

Incorporation of the biomass dynamics into the three-pool model produces the expectation of ecosystem total carbon (x):

$$E[x] = U \cdot \tau_E \cdot \frac{\lambda}{\lambda + s\tau_1}, \quad (9)$$

where τ_E is ecosystem carbon residence time (see detailed mathematical derivations in Appendix A, equations (A1)–(A14)). If the disturbance severity (s) is a random variable, the expectation of total ecosystem carbon (x) is:

$$E[x] = U \cdot \tau_E \cdot \frac{\lambda}{\lambda + E[s] \cdot \tau_1}, \quad (10)$$

where $E(s)$ is the expectation of disturbance severity (equations (A15)–(A17)).

[20] These equations constitute the REGIME model, which contains two parts, the potential C storage ($U\tau_E$) and the disturbance effect factor ($\frac{\lambda}{\lambda + E[s] \cdot \tau_1}$). The former is determined by ecosystem internal processes and the latter is determined by disturbance severity, mean disturbance intervals, and the residence time of the C pool that is affected by disturbances. If define a disturbance index (σ) as E(s)/λ, the fraction of biomass C removed by disturbance per unit of time, the equation is then written as $E[x] = U \cdot \tau_E \cdot \frac{1}{1+\sigma\tau_1}$. The model shows that carbon storage at a large spatial scale saturates with mean disturbance interval but decreases with disturbance severity (Figure 2a). The sensitivity of ecosystem C storage to disturbance is determined by the residence time of the C pool affected by disturbance (Figure 2b).

3.2. Sensitivity to PDFs of Disturbance Intervals and Recovery Patterns of NPP

[21] The sensitivity analyses showed the biases incurred by the assumptions of the independency of disturbance occurrence on ecosystem states (represented by the PDFs of disturbance intervals) and the recovery patterns of NPP were low when the mean disturbance interval was large (Figure 3). With equation (4), the simulated NPP increased in the first 10 years and then declined slightly, approaching its equilibrium state, around 1.2 Kg C m^{-2} $\cdot yr^{-1}$ (Figure 3a). The recovery patterns of the three C pools were similar at the two patterns of NPP (Figures 3b–3d). The mean carbon storages driven by this NPP pattern were similar with those at a constant NPP when the mean disturbance interval was longer than 20 yrs (Figure 3e). It indicated that the assumption of constant NPP resulted in very small biases in long-term. Only when the mean disturbance interval was shorter than 20 yrs, the simulated C content was lower than the predictions of the REGIME model (Figure 3e). The predicted ecosystem C storage by this model was not sensitive to the dependencies of disturbance on ecosystem states, which were represented by the shape factor k of the Weibull distribution when it varied from 1 to 2 (Figure 3f).

3.3. Comparison With the Simulations of TEM Model

[22] We compared the disturbance effects predicted by the REGIME model with those simulated by the TEM model (Figure 4). The ratios of vegetation (Figures 4a and 4c) and soil C storage (Figures 4b and 4d) to their corresponding potential values suggest this model captures key C dynamics. For the regions with low disturbance intervals (e.g., Canada), the simulated C content in vegetation and soil C pools are close to their potentials ($U\tau$); while, in the regions with frequent and severe disturbances, the C content is much lower than the potential (Figures 4a and 4b). The correlations between the ratios of actual to potential C content and the disturbance index (s/λ) of the 24 districts of the northern America follow the disturbance effect factor $\frac{1}{1+\sigma\cdot\tau_1}$ (Figures 4c and 4d).

4. Discussion

[23] The REGIME model is derived from the first principles of ecosystem C cycles and disturbance regimes. It predicts the mean ecosystem C storage at large spatial scales as a function of ecosystem internal properties and disturbance regimes by a Michaelis-Menten type equation (i.e., $v = V_{\max}\frac{[S]}{[S]+K_m}$, τ_1 and λ/s are corresponding to the K_m and [S], respectively). The Michaelis-Menten equation, which was

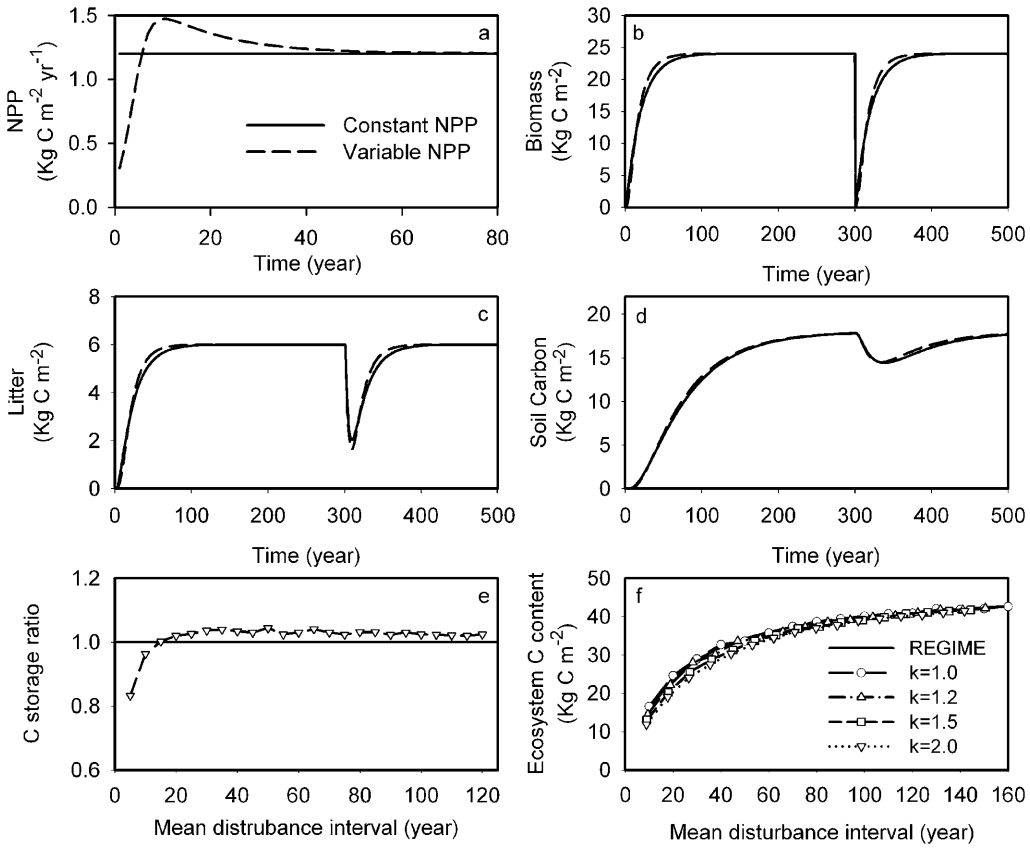

Figure 3. (a–e) Sensitivities of C storage to the recovery patterns of net primary production and (f) the probability distribution functions of disturbance intervals. Figure 3a shows the pattern of variable NPP generated using equation (3). Figures 3b–3d are the simulated carbon dynamics of (b) biomass, (c) litter, and (d) SOM at the two NPP patterns. The solid lines are simulations at constant NPP; the dashed lines are those at variable NPP. Figure 3e shows the ratios of simulated mean carbon content over 65,000 grids at variable NPP to that at constant NPP with mean disturbance intervals ranging from 5 to 120 years (dashed line with open triangle). In Figure 3f, the REGIME curve was generated using equation (9) with $U = 1.2$ Kg C $m^{-2} \cdot yr^{-1}$, τ_E = 40 yrs, τ_1 = 20 yrs, and s = 1.0. Other curves were the simulated mean carbon contents over 65,000 grids with disturbance intervals sampled in a Weibull distribution with shape factors (k) varying from 1.0 to 2.0.

first developed to describe enzyme kinetics, has been widely used in ecology, such as species richness [*Denslow*, 1995; *Keating and Quinn*, 1998], Predator-prey theory [*Berryman*, 1992], and animal growth [*Lopez et al.*, 2000]. Our mathematical derivation shows it can also be used in approximating ecosystem carbon storage with effects of disturbances.

[24] The model indicates that the sensitivity of carbon storage capacity to disturbances is determined by τ_1, the residence time of the pool that is directly affected by disturbances. For example, the C storage of forests is more sensitive to disturbances than it of grasslands since the woody biomass of trees has longer residence time and needs more time to recover than grasses. The C storage patterns represented by this model have been recognized by many observational and simulation studies [*Cooper*, 1983; *Dewar and Cannell*, 1992; *Harmon and Marks*, 2002; *Harmon et al.*, 1990; *Ryan and Williams*, 2011; *Smithwick et al.*, 2007]. Our analytical solution, based on the mathematical descriptions of ecosystem recovery patterns and disturbance regimes, illustrates how the deterministic ecosystem carbon processes and stochastic disturbance events interplay and therefore determine the C dynamics at long-term and large spatial scales.

4.1. Conceptualization of Ecosystem C Processes and Disturbance Regime

[25] This model is based on current knowledge of ecosystem recovery patterns and the probabilistic descriptions of disturbances, especially fires. Ecosystem C content usually decreases sharply at the occurrence of a large disturbance event and then gradually recovers, as being well documented by many chronosequence studies and long-term observations in most of the terrestrial biomes across the world [*Hughes et al.*, 1999; *Janisch and Harmon*, 2002; *Law et al.*, 2003; *Vargas et al.*, 2008]. The recovery patterns encompass the fluxes of ecosystem C input (i.e., NPP) and output (e.g., decompositions of litter and soil organic matters), controlled by ecosystem internal processes [*Law et al.*, 2003].

[26] At site level, the ecosystem C storage potential is a function of internal ecosystem processes (the product of NPP and residence time, $U\tau$). Over a large spatial scale, where disturbances are inevitable, the mean C storage is always

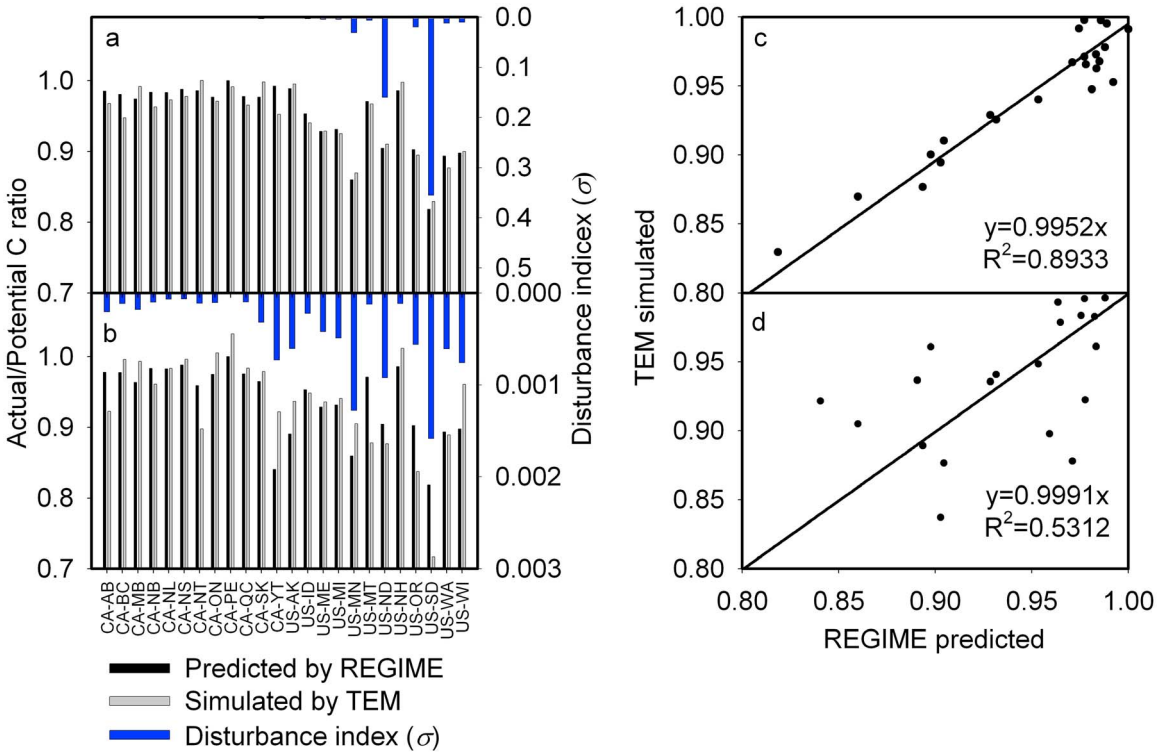

Figure 4. REGIME predicted and TEM simulated vegetation and soil C storage in the high-latitude regions of North America. (a, c) Vegetation C, (b, d) soil C. In Figures 4a and 4b the black bars are the ratios of REGIME predicted C content to the potential C storage calculated by the product of NPP and residence time. The gray bars are those of TEM simulated. The blue bars are disturbance indices for (a) vegetation or (b) soil C in the 24 regions. Figures 4c and 4d show the relationship between the ratios of REGIME predicted and TEM simulated C content to the potential C storage of vegetation and soil C pool, respectively.

lower than its potential capability ($U\tau$), since ecosystems are usually at different recovery stages as a consequence of random occurrence of disturbance events (Figures S1a and S1b in Text S1 in the auxiliary materials).[1] If the C content at a grid is taken as a sample of the C content in the disturbance-recovery curve, averaging over this curve is the same as averaging over a large homogenous region. So, the C storage capacity at a large spatial scale is the average of the C dynamics curve over an infinite time, becoming a function of ecosystem internal processes (U, τ) and disturbance regimes (λ, s) (Figure S1c in Text S1).

[27] Disturbances may affect different pools of an ecosystem directly or indirectly. For deriving the analytical solution, we just need one pool to represent the pools directly affected by disturbances and another one for the pools indirectly affected by disturbances (i.e., via the pools that are directly affected by disturbances). We used three pools in this study for being realistic: one pool that is directly affected by disturbances; and another two indirectly affected by disturbances. From the equations of ecosystem C storage (equations (9), (10), (A6), and (A14)), we can see that the number of C pools does not affect the final solution, but it does affect ecosystem properties and assumptions of disturbance impacts (e.g., C residence time and ecosystem-disturbance interactions). So, in future, we should evaluate how to accurately describe ecosystem responses to disturbances, though the assumptions in this study are acceptable for describing C storage dynamics at large scales.

[28] The assumptions about disturbance regimes and ecosystem C processes that are applied in deriving this model include (1) no effects of disturbance on NPP and residence times, (2) independence of the fraction of carbon removed by a disturbance event from current carbon content of biomass, and (3) exponential distribution of disturbance intervals, which is equivalent to the temporal independence of disturbance events. These assumptions highly simplify the complex system with diverse ecosystem-disturbance interactions while preserving their key characteristics (i.e., recovery patterns and PDFs of disturbance intervals), and allow us to get a meaningful analytical solution to describe the dynamics of C storage capacity as a function of ecosystem carbon processes (i.e., NPP and residence time) and disturbance regimes (represented by the mean frequency and severity of disturbance events).

[29] To examine the influences of these assumptions on model predictions, we tested the sensitivities of predicted C storage to alternative assumptions and compared the predictions of this model with the simulations of TEM model. Both the sensitivity analysis and model intercomparison demonstrate these assumptions are acceptable at large spatial scales and biases due to violating these assumptions are low given current disturbance regime.

[1] Auxiliary materials are available in the HTML. doi:10.1029/2012JG002040.

[30] The recovery periods of NPP for temperate and boreal forests are usually 5–20 years even after a stand-replacing disturbance (fires or harvests) [*Amiro et al.*, 2010; *Hicke et al.*, 2003; *Hughes et al.*, 1999; *Law et al.*, 2003], which are short in comparison to the long recovery time of carbon stocks (more than one century). Recovery patterns of the three C pools can be well approximated by the model regardless of the temporal changes in NPP (Figures 3b–3d). Fire disturbance regimes are usually determined by climatic conditions, such as temperature, drought, and wind, with weak effects of ecosystem properties, e.g., biomass and litters [*Baker*, 1989; *Romme et al.*, 2011; *Turner*, 2010]. The simulated carbon contents with disturbance intervals sampled from a Weibull distribution with shape factor $k = 2$, a high dependency on the fuel building up, are close to the REGIME predictions when the mean disturbance interval is longer than 80 years (Figure 3f). These tests indicate the key characteristics of ecosystem processes and disturbance regimes are kept in these assumptions, which makes the model be able to describe large-scale patterns of carbon cycles, though the model likely has insufficient detail to describe specific locations without additional parameters.

[31] The agreement between REGIME predictions and TEM simulations (Figure 4) also indicates that the assumptions are acceptable and the REGIME model is able to capture the key patterns of ecosystem carbon dynamics with effects of fires and harvests. These two models are independent with each other in representing the effects of disturbances on C dynamics. The TEM, as a simulation model, is driven by the detailed environmental conditions, e.g., temperature, precipitation, wind, solar radiation, soil moisture, etc., and all events of fires and harvests occurred in this region during the simulation period, and simulates the C dynamics of different ecosystem types at each $0.5^\circ \times 0.5^\circ$ grid of the high-latitude regions of North America. The REGIME model predicts large scale ecosystem C storage with the averaged characteristics of ecosystem properties and disturbance severities and frequencies. Therefore, the comparison to the simulations of TEM is an independent test of the REGIME model for its predictions of disturbance effects.

[32] The different agreements of predicted vegetation and soil C pools between these two models result from the differential rationales of the two models. As shown in the Figure 4, the agreement of biomass between these two models is good ($R^2 = 0.8933$ with a slope 0.9952), but for soil carbon the R^2 is 0.5321, much lower than that of biomass, though the slope is still close to 1 (0.9991). What the REGIME model predicts is the mean C content of a large spatial scale when the system is fully equilibrated with a disturbance regime; while the simulations of TEM are the time and space specific ecosystem states under the influences of recorded disturbance events. For the vegetation C pool, the regional average simulations are close to the conditions required by the REGIME model. But for the simulations of soil C pool, the long residence time and direct and indirect disturbance effects (as represented by equation (5)) make them deviate from the conditions of the REGIME model, and therefore the variations of the regional means from their theoretical predictions are high.

4.2. Application Perspectives

[33] The REGIME model provides a simple framework for representing ecosystem states and processes for modeling studies. Simulation models employ the similar types of assumptions for ecosystem processes, disturbances, and their interactions, with varied values or PDFs of the disturbance parameters, s, λ, and the disturbance transfer matrix Ξ in equation (2) and the recovery-related parameters in equation (3) (NPP and decomposition rates) [e.g., *Kurz and Apps*, 1994; *Smithwick et al.*, 2007; *Turner et al.*, 1993]. Our knowledge of these parameters is very limited though great insights have been gained via numerous field studies and observational networks in recent decades. The assumptions in this study fall in the ranges of aforementioned simulation studies, but make it possible to derive a simple but meaningful analytical solution, which, together with the mathematical expressions of ecosystem processes and disturbance regimes (equations (2) and (3)), can be used to analyze the simulation models.

[34] In most global modeling studies about terrestrial carbon dynamics, for example, the models are routinely initialized with the carbon pools equilibrated to historical climate data [*Hayes et al.*, 2011; *McGuire et al.*, 2001; *Schimel et al.*, 1997; *Sitch et al.*, 2008]. This is known to overestimate the initial terrestrial C storage. For example, C storage will be overestimated by approximately 20% if disturbance occurs once every 40 years on average with a severity of 0.5 according to this model. Lack of representation of disturbances in models also results in overestimation of terrestrial carbon sequestration in response to climate change, since the increases in disturbances can incur a large amount of carbon losses [*Schimel et al.*, 1997]. The REGIME model can be used to re-evaluate these model predictions with information of disturbance regimes.

[35] The REGIME model also provides a framework for the analysis of ecosystem carbon dynamics observed in small spatial and fine temporal scales (e.g., net ecosystem exchange from eddy-flux towers and inventories of forests). Old-growth forests, for example, were considered to be carbon neutral, which was usually defined as the state when net ecosystem production is zero [*Luyssaert et al.*, 2008; *Odum*, 1969]. Recent studies showing that old-growth forests are still sequestering C [*Lewis et al.*, 2009; *Luyssaert et al.*, 2008] seem to reject the hypothesis that the old-growth forest is C neutral. For most forest eddy-flux sites in North America, the NEE is negative, i.e., the forest is sequestrating C, even long time after a stand-replacing disturbance [*Amiro et al.*, 2010]. However, as a slow-in, fast-out system, most forest ecosystems may appear to be storing carbon at the time of measurement even they are actually C neutral since the odds of observing a "fast-out" C pulse are very low [*Kőrner*, 2003]. According to the REGIME model, the mean growth rate of the vegetation C pool (or net ecosystem exchange) is $U\frac{\sigma\cdot\tau_1}{1+\sigma\cdot\tau_1}$ ($\sigma = s/\lambda$) for a C-neutral ecosystem (for the derivation of this equation, see Appendix B). This amount of C is to counteract the C loss induced by randomly happened disturbance events. To provide a specific solution, the C storage will be constant when the mean net carbon influx is 100 g C m^{-2} yr^{-1} for a forest with 600 g C m^{-2} yr^{-1} of NPP, 20 yrs of biomass C residence time, in a disturbance regime with a 100 years' mean disturbance return interval and intensity ($NEP = U\frac{\sigma\cdot\tau_1}{1+\sigma\cdot\tau_1} = 600\cdot\frac{0.01\cdot 20}{1+0.01\cdot 20} = 100(\mathrm{g\,C\,m^{-2}yr^{-1}})$). The classic definition of C neutral happens only when ecosystem

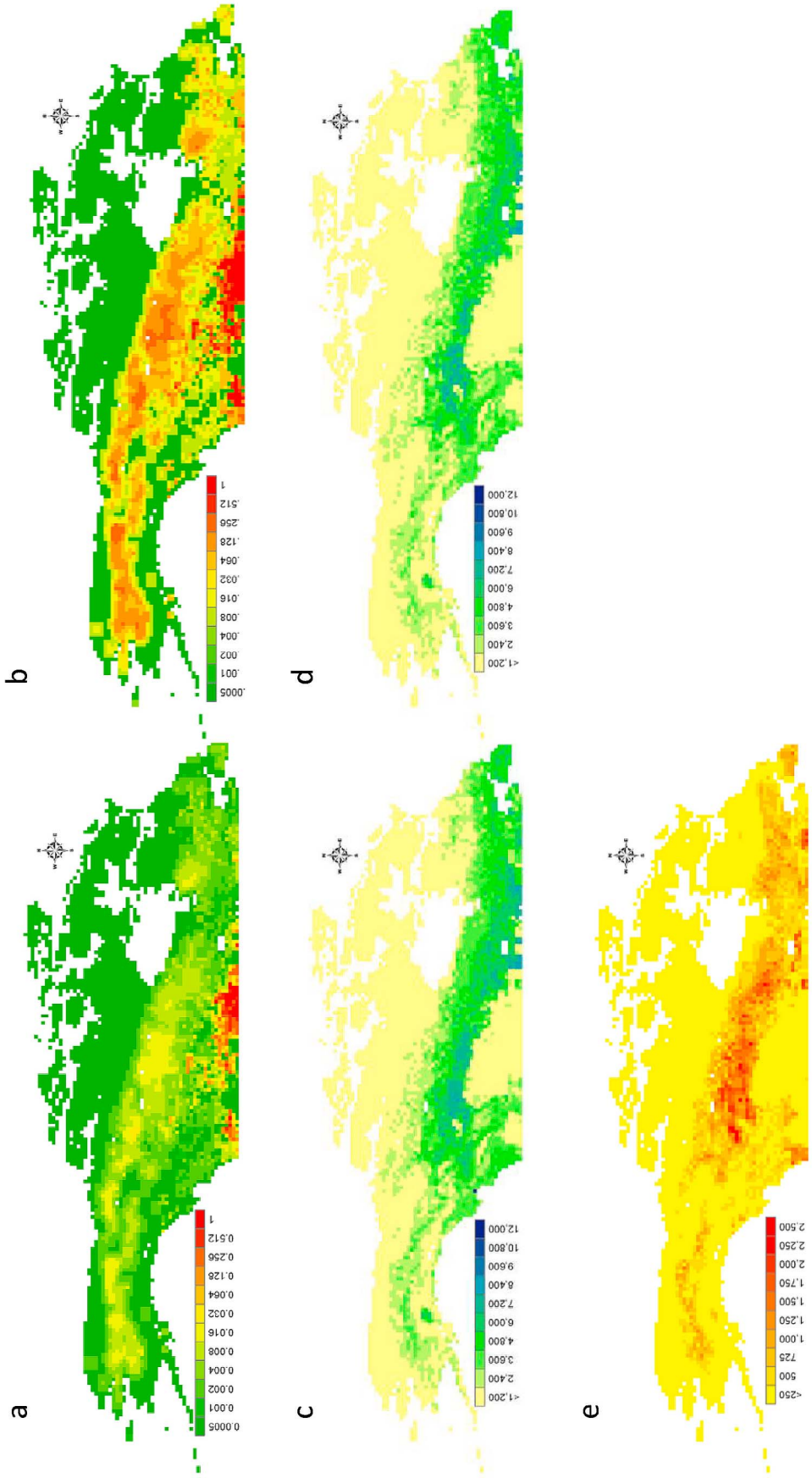

Figure 5. Vegetation carbon storage of high-latitude regions (>45°N) of North America at different disturbance regimes. (a) The current disturbance regime from *Balshi et al.* [2007], showing the fraction of vegetation C that is removed by fires and harvests per year. (b) The predicted disturbance regime in the last decade of the twenty-first century (5.7 times the current disturbance index, following *Balshi et al.* [2009]). (c) The current vegetation C storage (g C m^{-2}). (d) Vegetation C storage (g C m^{-2}) in the last decade of the twenty-first century with changes in disturbance calculated using equation (5). (e) The C losses of vegetation induced by changes in disturbance regimes.

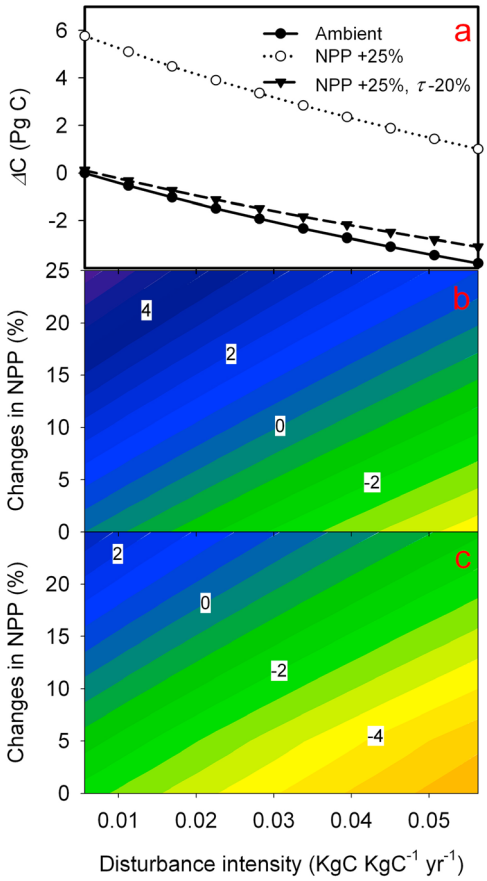

Figure 6. Ensemble analyses of changes in vegetation carbon storage in the high-latitude regions of North America. (a) The C-stock changes (Pg C) with disturbance intensity at ambient NPP and residence time (solid line with closed circles), 25% increases in NPP (dotted line with open circles), and 20% decreases in residence time (τ) with 25% increases in NPP (long-dashed line with closed triangles). (b, c) The isometric lines of vegetation C-stock changes with changes in NPP and disturbance intensity at (b) ambient and (c) 10% reduced residence times.

C content is at the potential maximum ($U\tau_E$) (or in the trivial case when NPP is zero) and no disturbance happens.

[36] The model allows us to get a sense of the sensitivity of ecosystems to future environmental changes just by a few calculations. In the high-latitude regions of North America, for example, if fire disturbance intensity increases around 5.7 time the current disturbance intensity (0.00563 Kg C Kg C^{-1} yr^{-1}) to the end of the twenty-first century as predicted by *Balshi et al.* [2009] (Figures 5a and 5b), approximately 1.8 Pg C will be lost given that NPP and residence time are constant according to the calculations of the REGIME model. The major carbon storage losses will occur in the boreal forest belt (Figures 5c–5e). This pattern and the C release amount are comparable with the simulated predictions of the TEM [*Balshi et al.*, 2009]. According to the REGIME, a 25% increase in NPP can compensate the C loss induced by an increase in the disturbance intensity from 0.00563 to 0.0563 Kg C Kg C^{-1} yr^{-1} (10 times the current disturbance intensity), while a 25% increase in NPP with a 20% decrease in residence time leaves the potential (equilibrium) vegetation C storage unchanged. The C losses induced by the same intensity of disturbances decrease, since the lowered residence time reduces the sensitivity of C storage to disturbance (Figure 6a). In this region, each change of current disturbance intensities (0.00563 Kg C Kg C^{-1} yr^{-1}) requires around 2% increases in NPP to keep the C storage at current level if residence times are not altered (Figure 6b). Thus, an increase of six times the current disturbance intensity, as predicted by *Balshi et al.* [2009], will require around 12% increases in NPP to maintain stable carbon stocks (Figure 6b). If the residence time decreased 10% at the same time (for example, if increasing temperature accelerates decomposition rates), this requires additional 12.5% increases in NPP to compensate. In this scenario, the required increase in NPP to maintain constant C storage will be more than 24% (Figure 6c). The chances of terrestrial ecosystems to maintain carbon sinks depend on how NPP, disturbance intensity and residence time respond to climate change. The REGIME allows us to explore the interdependence of these factors independent of the exact biological mechanisms in play and so can bound potential responses of terrestrial ecosystems to global change, as has been done by ensemble simulations [*Kurz et al.*, 2008a; *Metsaranta et al.*, 2010; *Metsaranta et al.*, 2011].

4.3. Model Uncertainties

[37] Caution must be taken when applying this model at finer scales or dealing with more complicated disturbance types and interactions. The assumptions used to derive this model define a dynamic equilibrium state at large spatial scale where ecosystems will eventually recover to their original states after disturbed [*Turner et al.*, 1993]. Therefore, the REGIME model only predicts the C storage dynamics of ecosystems at dynamic equilibrium states with disturbances. And, it does not deal with state shifts triggered by disturbance events [e.g., *Johnstone et al.*, 2010].

[38] The model shows that the mean fields of ecological and disturbance variables, e.g., NPP, decomposition/mortality rates, disturbance return intervals and severities, can be used to approximate large spatial scale carbon storage dynamics. But, the sensitivity tests indicate that the recovery patterns of NPP (Figure 3e) and the PDFs of disturbance intervals (Figure 3f) can substantially affect the estimation of ecosystem C storage when disturbance intervals are shortened, which likely happens with climate change [*Westerling et al.*, 2011]. The model predictions are likely to be biased by the complex interactions among residence time, NPP and disturbance severity when disturbance intervals are relatively short. And, the dependencies of disturbance severities on biomass conditions and the history of disturbances need to be carefully evaluated since the interactions among disturbances often shape disturbance-C storage dynamics (e.g., drought-insect-fire) [*Dale et al.*, 2001; *Miao et al.*, 2009].

[39] The conceptualization of the C processes and disturbance regimes in this study is useful for solving aforementioned problems. Further studies should be conducted to better understand the complex interactions between ecosystems and disturbance with varying assumptions. The stochastic representation of ecosystem processes and disturbance

effects in equation (2) presented by this study provides an ideal framework.

5. Conclusions

[40] In this study we present an analytical model to describe how ecosystem carbon storage is determined by NPP, C residence time, and disturbance interval and severity. It integrates the deterministic ecosystem carbon processes and stochastic disturbance events in a tractable mathematical model. A couple of key assumptions are applied in the conceptualization of the ecosystem processes, disturbance regimes, and disturbance effects for mathematically representations of ecosystem-disturbance interactions. This model provides a framework for the analysis of ecosystem carbon dynamics observations at site scales and a tool of representing ecosystem states and processes for large scale modeling studies. Further studies are needed to the development of a more sophisticated model describing complicated interactions among ecological processes and disturbances. This model, together with its assumptions, lays the foundation for the future studies of analytically modeling the interactions between deterministic biogeochemical processes and stochastic disturbance events.

Appendix A: Mathematical Derivations of the REGIME Model

[41] The ecosystem carbon (C) cycle model (conceptual BGC model) is described by the following equation:

$$\frac{dX(t)}{dt} = AR^{-1}X(t) + BU(t), \tag{A1}$$

where $X(t)$ is ecosystem carbon content at time t, A is a 3×3 matrix representing carbon transfer among the three pools, $A = \begin{pmatrix} -1 & 0 & 0 \\ 1 & -1 & 0 \\ 0 & \eta & -1 \end{pmatrix}$, and η is the ratio of carbon transferred to the SOM pool from the litter pool. T is a 3×3 diagonal matrix, $R = diag(\tau)$. The diagonal elements, τ_1, τ_2, and τ_3, are the residence times of the carbon in biomass, litter, and SOM, respectively. B is the vector allocation ratios of carbon input to the three pools, $(1 \quad 0 \quad 0)'$. $U(t)$ is the carbon input (NPP) at time t. We assumed it was a constant in model simulations and mathematical derivations.

A1. Carbon Storage Capacity at the Disturbances, With Severity Being 1.0

[42] According to equation (A1), the carbon content of biomass with an initial value of zero follows the following equation:

$$X_1 = U\tau_1\left(1 - e^{-t/\tau_1}\right), \tag{A2}$$

where t is time.

[43] For each disturbance cycle, the mean C content over a disturbance interval T can be taken as the height of a rectangle with the length T and the same area with that enclosed by the recovery cure (Figure S2a in Text S1 in the auxiliary materials). Thus, the mean carbon content of biomass ($X_{1,\text{avg}}$) in a disturbance cycle with interval T:

$$X_{1,avg} = \frac{\left[\int_0^T U\tau_1\left(1 - e^{-\frac{t}{\tau_1}}\right)dt\right]}{T} = U\tau_1 \cdot \left[1 - \frac{\tau_1}{T} \cdot \left(1 - e^{-\frac{T}{\tau_1}}\right)\right]. \tag{A3}$$

Note, the interval T is in distribution:

$$f(T;\lambda) = \begin{cases} \frac{1}{\lambda} \cdot e^{-\frac{1}{\lambda}T}, T \geq 0 \\ 0 \qquad\quad , T < 0 \end{cases}. \tag{A4}$$

The mean carbon content in an infinite time series with numerous disturbance events can be calculated as the total area enclosed by the recovery curves divided by the sum of T's. Taking the probability density function of interval T into account, the mean carbon content is:

$$\begin{aligned} E[X_1] &= \frac{\int_0^\infty T \cdot U\tau_1 \cdot \left[1 - \frac{\tau_1}{T} \cdot \left(1 - e^{-\frac{T}{\tau_1}}\right)\right] \cdot \frac{1}{\lambda} \cdot e^{-\frac{1}{\lambda}T} dT}{\int_0^\infty T \cdot \frac{1}{\lambda} \cdot e^{-\frac{1}{\lambda}T} dT} \\ &= U\tau_1 \frac{\lambda}{\lambda + \tau_1}. \end{aligned} \tag{A5}$$

For the pools of litter and SOM, the changes are only their inputs. For a long period, the whole ecosystem carbon content (x) can be represented by:

$$\begin{aligned} E[x] &= E[X_1] + E[X_2] + E[X_3] \\ &= U\tau_1 \cdot \frac{\lambda}{\lambda + \tau_1} + \frac{E[X_1]}{\tau_1} \cdot \tau_2 + \frac{E[X_2]}{\tau_2} \cdot \eta \cdot \tau_3 \\ &= U\tau_1 \cdot \frac{\lambda}{\lambda + \tau_1} + U\tau_1 \cdot \frac{\lambda}{\lambda + \tau_1} \cdot \frac{1}{\tau_1} \cdot \tau_2 + U\tau_1 \\ &\quad \cdot \frac{\lambda}{\lambda + \tau_1} \cdot \frac{1}{\tau_1} \cdot \tau_2 \cdot \frac{1}{\tau_2} \cdot \eta \cdot \tau_3 = U(\tau_1 + \tau_2 + \tau_3 \cdot \eta) \cdot \frac{\lambda}{\lambda + \tau_1} \\ &= U\tau_E \cdot \frac{\lambda}{\lambda + \tau_1}. \end{aligned} \tag{A6}$$

A2. Carbon Storage Capacity at the Disturbances, With Severity Less Than 1.0

[44] For each disturbance cycle, the carbon can be divided into two parts: the legacy carbon from the last rotation, the new carbon accumulated from zero since the disturbance event (see Figure S2b). The legacy carbon decomposes exponentially ($X_{1,old} = x_{1,0} \cdot e^{-t/\tau_1}$, where $x_{1,0}$ is the initial value of legacy carbon just after a disturbance event); the new carbon accumulates following the equation $X_{1,new} = U\tau_1(1 - e^{-t/\tau_1})$, the total carbon of biomass at time t since last disturbance is:

$$X_1 = U\tau_1\left(1 - e^{-t/\tau_1}\right) + x_{1,0} \cdot e^{-t/\tau_1}. \tag{A7}$$

The mean carbon content of biomass in a disturbance rotation ($X_{1,avg}$) with given $x_{1,0}$ and disturbance interval T:

$$X_{1,avg} = \left[\int_0^T U\tau_1\left(1-e^{-\frac{t}{\tau_1}}\right)dt + \int_0^T x_{1,0}\cdot e^{-t/\tau_1}dt\right]/T = U\cdot\tau_1\cdot\left[1-\frac{\tau_1}{T}\cdot\left(1-e^{-\frac{T}{\tau_1}}\right)\right] + x_{1,0}\cdot\frac{\tau_1}{T}\cdot\left(1-e^{-\frac{T}{\tau_1}}\right). \tag{A8}$$

Since $x_{1,0}$ is determined by the previous disturbance event, it is independent of the interval of the next disturbance, T. Thus, considering the exponential probability distribution of disturbance intervals, the expectation of this rotation conditioned on $x_{1,0}$ is:

$$E\left[X_1|x_{1,0}\right] = \frac{\int_0^\infty T\cdot U\cdot\tau_1\cdot\left[1-\frac{\tau_1}{T}\cdot\left(1-e^{-\frac{T}{\tau_1}}\right)\right]\cdot\frac{1}{\lambda}\cdot e^{-\frac{1}{\lambda}T}dT + \int_0^\infty T\cdot x_{1,0}\cdot\frac{\tau_1}{T}\cdot\left(1-e^{-\frac{T}{\tau_1}}\right)\cdot\frac{1}{\lambda}\cdot e^{-\frac{1}{\lambda}T}dT}{\int_0^\infty T\cdot\frac{1}{\lambda}\cdot e^{-\frac{1}{\lambda}T}dT} = U\tau_1\cdot\frac{\lambda}{\lambda+\tau_1} + x_{1,0}\cdot\frac{\tau_1}{\lambda+\tau_1}. \tag{A9}$$

Then, the expectation of X_1 is:

$$E[X_1] = E\left[E\left[X_1|x_{1,0}\right]\right] = E\left[U\tau_1\cdot\frac{\lambda}{\lambda+\tau_1} + x_{1,0}\cdot\frac{\tau_1}{\lambda+\tau_1}\right] = U\tau_1\cdot\frac{\lambda}{\lambda+\tau_1} + E\left[x_{1,0}\right]\cdot\frac{\tau_1}{\lambda+\tau_1}. \tag{A10}$$

For solving the mean of $x_{1,0}$, we need to know the mean of the carbon content just before disturbance happens ($X_{1,0}^-$) ($X_{1,0}^- = x_{1,0}\cdot e^{-t/\tau_1} + U\tau_1(1-e^{-t/\tau_1})$, where $x_{1,0}$ is the initial value of that disturbance cycle) (see Figure S2c for the definition of X_1, $X_{1,0}^-$, and $x_{1,0}$). Let t be the time that the disturbance happens since the last one. The distribution of t is an exponential distribution:

$$\begin{aligned}E\left[X_{1,0}^-\right] &= E\left[x_{1,0}\cdot e^{-t/\tau_1}\right] + E\left[U\tau_1\left(1-e^{-t/\tau_1}\right)\right]\\ &= E\left[x_{1,0}\right]\frac{1}{\lambda}\int_{t=0}^{t=\infty} e^{-t/\tau_1}\cdot e^{-\frac{1}{\lambda}t}dt + \frac{1}{\lambda}U\tau_1\int_{t=0}^{t=\infty} e^{-\frac{1}{\lambda}t}dt - \frac{1}{\lambda}U\tau_1\int_{t=0}^{t=\infty} e^{-t/\tau_1}\cdot e^{-\frac{1}{\lambda}t}dt\\ &= E\left[x_{1,0}\right]\frac{1}{\lambda}\int_{t=0}^{t=\infty} e^{-t/\tau_1}\cdot e^{-\frac{1}{\lambda}t}dt + \frac{1}{\lambda}U\tau_1\int_{t=0}^{t=\infty} e^{-\frac{1}{\lambda}t}dt - \frac{1}{\lambda}U\tau_1\int_{t=0}^{t=\infty} e^{-t/\tau_1}\cdot e^{-\frac{1}{\lambda}t}dt\\ &= \left(\frac{E\left[x_{1,0}\right]}{\lambda} - \frac{U\tau_1}{\lambda}\right)\int_{t=0}^{t=\infty} e^{-\left(\frac{1}{\lambda}+\frac{1}{\tau_1}\right)t}dt + \frac{1}{\lambda}U\tau_1\cdot\int_{t=0}^{t=\infty} e^{-\frac{1}{\lambda}t}dt\\ &= \left(\frac{E\left[x_{1,0}\right]}{\lambda} - \frac{U\tau_1}{\lambda}\right)\cdot\frac{\lambda\tau}{\lambda+\tau} + U\tau_1\\ &= E\left[x_{1,0}\right]\cdot\frac{\tau_1}{\lambda+\tau_1} + U\tau_1\cdot\frac{\lambda}{\lambda+\tau_1}.\end{aligned} \tag{A11}$$

It indicates that $E[X_{1,0}^-] = E[X_1]$.

[45] For each $X_{1,0}^-$ there is an $x_{1,0} = (1-s)\cdot X_{1,0}^-$. Thus,

$$\bar{x}_{1,0} = (1-s)E\left[X_{1,0}^-\right] = (1-s)\left[\bar{x}_{1,0}\cdot\frac{\tau_1}{\lambda+\tau_1} + U\tau_1\cdot\frac{\lambda}{\lambda+\tau_1}\right] \Rightarrow \bar{x}_{1,0} = (1-s)\cdot U\tau_1\cdot\frac{1}{1+s\tau_1/\lambda}. \tag{A12}$$

Therefore, the expectation of X_1 (plant biomass) in a disturbance regime with severity s and mean interval λ is:

$$\begin{aligned}E[X_1] &= U\tau_1\cdot\frac{\lambda}{\lambda+\tau_1} + E\left[x_{1,0}\right]\cdot\frac{\tau_1}{\lambda+\tau_1}\\ &= U\tau_1\cdot\frac{\lambda}{\lambda+\tau_1} + (1-s)\cdot U\tau_1\cdot\frac{\lambda}{\lambda+s\tau_1}\cdot\frac{\tau_1}{\lambda+\tau_1}\\ &= U\tau_1\cdot\left[\frac{\lambda}{\lambda+\tau_1} + \frac{(1-s)\cdot\lambda}{\lambda+s\tau_1}\cdot\frac{\tau_1}{\lambda+\tau_1}\right]\\ &= U\tau_1\cdot\frac{1}{\lambda+\tau_1}\cdot\left[\lambda + \frac{(1-s)\cdot\lambda}{\lambda+s\tau_1}\cdot\tau_1\right]\\ &= U\tau_1\cdot\frac{1}{\lambda+\tau_1}\cdot\left[\frac{(\lambda+\tau_1)\cdot\lambda}{\lambda+s\tau_1}\right]\\ &= U\cdot\tau_1\cdot\frac{\lambda}{\lambda+s\tau_1}.\end{aligned} \tag{A13}$$

And, for the expectation of ecosystem total carbon (X):

$$\begin{aligned}E[x] &= E[X_1] + E[X_2] + E[X_3]\\ &= U\tau_1\cdot\frac{\lambda}{\lambda+\tau_1} + \frac{E[X_1]}{\tau_1}\cdot\tau_2 + \frac{E[X_2]}{\tau_2}\cdot\eta\cdot\tau_3\\ &= U\tau_1\cdot\frac{\lambda}{\lambda+s\tau_1} + U\tau_1\cdot\frac{\lambda}{\lambda+s\tau_1}\cdot\frac{1}{\tau_1}\cdot\tau_2 + U\tau_1\cdot\frac{\lambda}{\lambda+s\tau_1}\cdot\frac{1}{\tau_1}\cdot\tau_2\cdot\frac{1}{\tau_2}\cdot\eta\cdot\tau_3\\ &= U\tau_1\cdot\frac{\lambda}{\lambda+s\tau_1} + U\tau_2\cdot\frac{\lambda}{\lambda+s\tau_1} + U\tau_3\cdot\eta\cdot\frac{\lambda}{\lambda+s\tau_1}\\ &= U(\tau_1+\tau_2+\tau_3\cdot\eta)\cdot\frac{\lambda}{\lambda+s\tau_1}\\ &= U\tau_E\cdot\frac{\lambda}{\lambda+s\tau_1}.\end{aligned} \tag{A14}$$

[46] According to equation (A14), ecosystem carbon storage capacity can be estimated by its intrinsic properties (U and τ) and disturbance regime (λ and s). We also

simulated carbon storage capacities with severities (s) ranging from 0 to 1. The agreement between the predictions of the analytical model (REGIME) and the simulations of the conceptual BGC model is shown in Figures S3a and S3b. The agreement between the mean of carbon content just after disturbance events calculated using equation (A12) and the simulations of the conceptual BGC model is shown in Figure S3c.

A3. When Disturbance Severity is a Random Variable

[47] If severity (s) is a random variable in [0,1], then the mean carbon content can be calculated as following.

[48] As we have known, the expectation of X_1 and $X_{1,0}^-$ is $E(X_1) = E\left[X_1^-\right] = U\tau_1 \cdot \frac{\lambda}{\lambda+\tau_1} + E\left[x_{1,0}\right] \cdot \frac{\tau_1}{\lambda+\tau_1}$.

[49] And, for each $X_{1,0}^-$, there is an $x_{1,0} = (1 - s) \cdot X_{1,0}^-$. Thus,

$$\begin{aligned} E\left[x_{1,0}\right] &= E[(1-s)]E\left[X_{1,0}^-\right] = (1-E[s]) \\ &\quad \cdot \left[\bar{x}_{1,0} \cdot \frac{\tau_1}{\lambda+\tau_1} + U\tau_1 \cdot \frac{\lambda}{\lambda+\tau_1}\right] \\ &\Rightarrow E\left[x_{1,0}\right] = (1-E[s]) \cdot U\tau_1 \cdot \frac{1}{1+E[s]\cdot\tau_1/\lambda}. \end{aligned} \tag{A15}$$

Therefore, the expectation of X_1 is:

$$\begin{aligned} E[X_1] &= U\tau_1 \cdot \frac{1}{1+E[s]\cdot\tau_1/\lambda} \\ &= U\tau_1 \cdot \frac{\lambda}{\lambda+E[s]\cdot\tau_1}. \end{aligned} \tag{A16}$$

And, the expectation of total ecosystem carbon (x) is:

$$E[x] = U\tau_E \cdot \frac{\lambda}{\lambda+E[s]\cdot\tau_1}. \tag{A17}$$

The agreement of the carbon contents calculated by this equation (A17) and the simulations of the conceptual BGC model is shown in Figure S3d.

Appendix B: Net Ecosystem Exchange (NEE) of C-Neutral Ecosystems Under the Influence of Disturbances

[50] For the ecosystems represented by our three-pool C cycle model (conceptual BGC), the heterotrophic respiration (R_h) is contributed by the litter (X_2) and the soil (X_3) carbon pools.

$$\begin{aligned} R_h &= (1-\eta)\cdot X_2/\tau_2 + X_3/\tau_3 \\ &= (1-\eta)\cdot U\tau_2 \cdot \frac{\lambda}{\lambda+s\tau_1}/\tau_2 + U\tau_3 \cdot \eta \cdot \frac{\lambda}{\lambda+s\tau_1}/\tau_3 \\ &= (1-\eta)\cdot U \cdot \frac{\lambda}{\lambda+s\tau_1} + U\cdot\eta\cdot\frac{\lambda}{\lambda+s\tau_1} \\ &= (1-\eta+\eta)\cdot U\cdot\frac{\lambda}{\lambda+s\tau_1} \\ &= U\cdot\frac{\lambda}{\lambda+s\tau_1}. \end{aligned} \tag{B1}$$

NEP is the difference between net primary production (U) and heterotrophic respiration (R_h):

$$\begin{aligned} NEP &= U - R_h \\ &= U - U\cdot\frac{\lambda}{\lambda+s\tau_1} \\ &= U\cdot\frac{s\tau_1}{\lambda+s\tau_1}. \end{aligned} \tag{B2}$$

Let $\sigma = s/\lambda$, then

$$\begin{aligned} NEP &= U\cdot\frac{s\tau_1}{\lambda+s\tau_1} \\ &= U\cdot\frac{s/\lambda\tau_1}{1+s/\lambda\tau_1} \\ &= U\cdot\frac{\sigma\tau_1}{1+\sigma\tau_1}. \end{aligned} \tag{B3}$$

[51] **Acknowledgments.** This research was financially supported by the Office of Science, Department of Energy (grant DE-FG02-006ER64319); by the Midwestern Regional Center of the National Institute for Climatic Change Research at Michigan Technological University under award DE-FC02-06ER64158; and by the National Science Foundation under DBI 0850290, DEB 0840964, DEB 0743778, and EPS 0919466. We thank Nikola P. Petrov of the University of Oklahoma, Jeremy W. Lichstein of the University of Florida, and Anping Chen of Princeton University for their helpful comments.

References

Amiro, B. D., et al. (2010), Ecosystem carbon dioxide fluxes after disturbance in forests of North America, *J. Geophys. Res.*, *115*, G00K02, doi:10.1029/2010JG001390.

Baker, W. L. (1989), Effect of scale and spatial heterogeneity on fire-interval distributions, *Can. J. For. Res.*, *19*, 700–706, doi:10.1139/x89-109.

Baker, W. L. (2009), *Fire Ecology in Rocky Mountain Landscapes*, Island Press, Washington, D. C.

Baker, W. L., and D. Ehle (2001), Uncertainty in surface-fire history: The case of ponderosa pine forests in the western United States, *Can. J. For. Res.*, *31*, 1205–1226, doi:10.1139/x01-046.

Balshi, M. S., et al. (2007), The role of historical fire disturbance in the carbon dynamics of the pan-boreal region: A process-based analysis, *J. Geophys. Res.*, *112*, G02029, doi:10.1029/2006JG000380.

Balshi, M. S., A. D. McGuire, P. Duffy, M. Flannigan, D. W. Kicklighter, and J. Melillo (2009), Vulnerability of carbon storage in North American boreal forests to wildfires during the 21st century, *Global Change Biol.*, *15*, 1491–1510, doi:10.1111/j.1365-2486.2009.01877.x.

Berryman, A. A. (1992), The origins and evolution of predator prey theory, *Ecology*, *73*, 1530–1535, doi:10.2307/1940005.

Bond-Lamberty, B., S. D. Peckham, D. E. Ahl, and S. T. Gower (2007), Fire as the dominant driver of central Canadian boreal forest carbon balance, *Nature*, *450*, 89–92, doi:10.1038/nature06272.

Bowman, D., et al. (2009), Fire in the Earth system, *Science*, *324*(5926), 481–484, doi:10.1126/science.1163886.

Clark, J. S. (1990), Fire and climate change during the last 750 yr in northwestern Minnesota, *Ecol. Monogr.*, *60*, 135–159, doi:10.2307/1943042.

Cooper, C. F. (1983), Carbon storage in managed forests, *Can. J. For. Res.*, *13*, 155–166, doi:10.1139/x83-022.

Dale, V. H., et al. (2001), Climate change and forest disturbances, *BioScience*, *51*, 723–734, doi:10.1641/0006-3568(2001)051[0723:CCAFD]2.0.CO;2.

Denslow, J. S. (1995), Disturbance and diversity in tropical rain-forests: The density effect, *Ecol. Appl.*, *5*, 962–968, doi:10.2307/2269347.

Dewar, R. C., and M. G. R. Cannell (1992), Carbon sequestration in the trees, products and soils of forest plantations: An analysis using UK examples, *Tree Physiol.*, *11*, 49–71.

Drobot, S., J. Maslanik, U. C. Herzfeld, C. Fowler, and W. L. Wu (2006), Uncertainty in temperature and precipitation datasets over terrestrial regions of the Western Arctic, *Earth Interact.*, *10*, 1–17, doi:10.1175/EI191.1.

Emanuel, K. (2005), Increasing destructiveness of tropical cyclones over the past 30 years, *Nature*, *436*, 686–688, doi:10.1038/nature03906.

Goetz, S. J., M. C. Mack, K. R. Gurney, J. T. Randerson, and R. A. Houghton (2007), Ecosystem responses to recent climate change and fire disturbance at northern high latitudes: Observations and model results contrasting northern Eurasia and North America, *Environ. Res. Lett.*, *2*, 045031, doi:10.1088/1748-9326/2/4/045031.

Gower, S. T., R. E. McMurtrie, and D. Murty (1996), Aboveground net primary production decline with stand age: Potential causes, *Trends Ecol. Evol.*, *11*, 378–382, doi:10.1016/0169-5347(96)10042-2.

Grissino-Mayer, H. D. (1999), Modeling fire interval data from the American Southwest with the Weibull distribution, *Int. J. Wildland Fire*, *9*, 37–50, doi:10.1071/WF99004.

Hamilton, J. G., E. H. DeLucia, K. George, S. L. Naidu, A. C. Finzi, and W. H. Schlesinger (2002), Forest carbon balance under elevated CO_2, *Oecologia*, *131*, 250–260, doi:10.1007/s00442-002-0884-x.

Harmon, M. E., and B. Marks (2002), Effects of silvicultural practices on carbon stores in Douglas-fir-western hemlock forests in the Pacific Northwest, USA: Results from a simulation model, *Can. J. For. Res.*, *32*, 863–877, doi:10.1139/x01-216.

Harmon, M. E., W. K. Ferrell, and J. F. Franklin (1990), Effects on carbon storage of conversion of old-growth forests to young forests, *Science*, *247*, 699–702, doi:10.1126/science.247.4943.699.

Hayes, D. J., A. D. McGuirez, D. W. Kicklighter, K. R. Gurney, T. J. Burnside, and J. M. Melillo (2011), Is the northern high-latitude land-based CO_2 sink weakening?, *Global Biogeochem. Cycles*, *25*, GB3018, doi:10.1029/2010GB003813.

Hicke, J. A., G. P. Asner, E. S. Kasischke, N. H. F. French, J. T. Randerson, G. J. Collatz, B. J. Stocks, C. J. Tucker, S. O. Los, and C. B. Field (2003), Postfire response of North American boreal forest net primary productivity analyzed with satellite observations, *Global Change Biol.*, *9*, 1145–1157, doi:10.1046/j.1365-2486.2003.00658.x.

Hughes, R. F., J. B. Kauffman, and V. J. Jaramillo (1999), Biomass, carbon, and nutrient dynamics of secondary forests in a humid tropical region of Mexico, *Ecology*, *80*, 1892–1907.

Janisch, J. E., and M. E. Harmon (2002), Successional changes in live and dead wood carbon stores: Implications for net ecosystem productivity, *Tree Physiol.*, *22*, 77–89, doi:10.1093/treephys/22.2-3.77.

Johnson, E. A., and S. L. Gutsell (1994), Fire frequency models, methods and interpretations, *Adv. Ecol. Res*, *25*, 239–287, doi:10.1016/S0065-2504(08)60216-0.

Johnstone, J. F., F. S. Chapin, T. N. Hollingsworth, M. C. Mack, V. Romanovsky, and M. Turetsky (2010), Fire, climate change, and forest resilience in interior Alaska, *Can. J. For. Res.*, *40*, 1302–1312, doi:10.1139/X10-061.

Kashian, D. M., M. G. Turner, W. H. Romme, and C. G. Lorimer (2005), Variability and convergence in stand structural development on a fire-dominated subalpine landscape, *Ecology*, *86*, 643–654, doi:10.1890/03-0828.

Kashian, D. M., W. H. Romme, D. B. Tinker, M. G. Turner, and M. G. Ryan (2006), Carbon storage on landscapes with stand-replacing fires, *BioScience*, *56*, 598–606, doi:10.1641/0006-3568(2006)56[598:CSOLWS]2.0.CO;2.

Katz, R. W., G. S. Brush, and M. B. Parlange (2005), Statistics of extremes: Modeling ecological disturbances, *Ecology*, *86*(5), 1124–1134, doi:10.1890/04-0606.

Keating, K. A., and J. F. Quinn (1998), Estimating species richness: The Michaelis-Menten model revisited, *Oikos*, *81*, 411–416, doi:10.2307/3547060.

Keeling, C. D., and T. P. Whorf (2005), *Atmospheric CO_2* Records From Sites in the SIO Air Sampling Network, CDIAC/Oak Ridge Natl. Lab., Oak Ridge, Tenn.

Kőrner, C. (2003), Slow in, rapid out–carbon flux studies and Kyoto targets, *Science*, *300*, 1242–1243, doi:10.1126/science.1084460.

Kurz, W. A., and M. J. Apps (1994), The carbon budget of Canadian forests: A sensitivity analysis of changes in disturbance regimes, growth-rates, and decomposition rates, *Environ. Pollut.*, *83*, 55–61, doi:10.1016/0269-7491(94)90022-1.

Kurz, W. A., and M. J. Apps (1999), A 70-year retrospective analysis of carbon fluxes in the Canadian forest sector, *Ecol. Appl.*, *9*, 526–547, doi:10.1890/1051-0761(1999)009[0526:AYRAOC]2.0.CO;2.

Kurz, W. A., G. Stinson, and G. Rampley (2008a), Could increased boreal forest ecosystem productivity offset carbon losses from increased disturbances?, *Philos. Trans. R. Soc. B*, *363*, 2259–2268, doi:10.1098/rstb.2007.2198.

Kurz, W. A., G. Stinson, G. J. Rampley, C. C. Dymond, and E. T. Neilson (2008b), Risk of natural disturbances makes future contribution of Canada's forests to the global carbon cycle highly uncerain, *Proc. Natl. Acad. Sci. U. S. A.*, *105*, 1551–1555, doi:10.1073/pnas.0708133105.

Kurz, W. A., C. C. Dymond, G. Stinson, G. J. Rampley, E. T. Neilson, A. L. Carroll, T. Ebata, and L. Safranyik (2008c), Mountain pine beetle and forest carbon feedback to climate change, *Nature*, *452*, 987–990, doi:10.1038/nature06777.

Law, B. E., O. J. Sun, J. Campbell, S. Van Tuyl, and P. E. Thornton (2003), Changes in carbon storage and fluxes in a chronosequence of ponderosa pine, *Global Change Biol.*, *9*, 510–524, doi:10.1046/j.1365-2486.2003.00624.x.

Lewis, S. L., et al. (2009), Increasing carbon storage in intact African tropical forests, *Nature*, *457*, 1003–1006, doi:10.1038/nature07771.

Lopez, S., J. France, W. J. J. Gerrits, M. S. Dhanoa, D. J. Humphries, and J. Dijkstra (2000), A generalized Michaelis-Menten equation for the analysis of growth, *J. Anim. Sci.*, *78*, 1816–1828.

Luo, Y. Q., and E. S. Weng (2011), Dynamic disequilibrium of the terrestrial carbon cycle under global change, *Trends Ecol. Evol.*, *26*, 96–104, doi:10.1016/j.tree.2010.11.003.

Luo, Y. Q., L. W. White, J. G. Canadell, E. H. DeLucia, D. S. Ellsworth, A. C. Finzi, J. Lichter, and W. H. Schlesinger (2003), Sustainability of terrestrial carbon sequestration: A case study in Duke Forest with inversion approach, *Global Biogeochem. Cycles*, *17*(1), 1021, doi:10.1029/2002GB001923.

Luyssaert, S., E. D. Schulze, A. Borner, A. Knohl, D. Hessenmoller, B. E. Law, P. Ciais, and J. Grace (2008), Old-growth forests as global carbon sinks, *Nature*, *455*, 213–215, doi:10.1038/nature07276.

McGuire, A. D., et al. (2001), Carbon balance of the terrestrial biosphere in the twentieth century: Analyses of CO_2, climate and land use effects with four process-based ecosystem models, *Global Biogeochem. Cycles*, *15*, 183–206, doi:10.1029/2000GB001298.

McGuire, A. D., et al. (2010), An analysis of the carbon balance of the Arctic Basin from 1997 to 2006, *Tellus, Ser. B*, *62*, 455–474, doi:10.1111/j.1600-0889.2010.00497.x.

Metsaranta, J. M., W. A. Kurz, E. T. Neilson, and G. Stinson (2010), Implications of future disturbance regimes on the carbon balance of Canada's managed forest (2010–2100), *Tellus, Ser. B*, *62*, 719–728, doi:10.1111/j.1600-0889.2010.00487.x.

Metsaranta, J. M., C. C. Dymond, W. A. Kurz, and D. L. Spittlehouse (2011), Uncertainty of 21st-century growing stocks and GHG balance of forests in British Columbia, Canada resulting from potential climate change impacts on ecosystem processes, *For. Ecol. Manage.*, *262*, 827–837, doi:10.1016/j.foreco.2011.05.016.

Miao, S. L., C. B. Zou, and D. D. Breshears (2009), Vegetation responses to extreme hydrological events: Sequence matters, *Am. Nat.*, *173*, 113–118, doi:10.1086/593307.

Mitchell, T. D., and P. D. Jones (2005), An improved method of constructing a database of monthly climate observations and associated high-resolution grids, *Int. J. Climatol.*, *25*, 693–712, doi:10.1002/joc.1181.

Odum, E. P. (1969), Strategy of ecosystem development, *Science*, *164*, 262–270, doi:10.1126/science.164.3877.262.

Parton, W. J., et al. (1993), Observations and modeling of biomass and soil organic-matter dynamics for the grassland biome worldwide, *Global Biogeochem. Cycles*, *7*, 785–809, doi:10.1029/93GB02042.

Potter, C. S., and S. A. Klooster (1997), Global model estimates of carbon and nitrogen storage in litter and soil pools: Response to changes in vegetation quality and biomass allocation, *Tellus, Ser. B*, *49*, 1–17, doi:10.1034/j.1600-0889.49.issue1.1.x.

Raich, J. W., E. B. Rastetter, J. M. Melillo, D. W. Kicklighter, P. A. Steudler, B. J. Peterson, A. L. Grace, B. Moore, and C. J. Vorosmarty (1991), Potential net primary productivity in South America: Application of a global model, *Ecol. Appl.*, *1*, 399–429, doi:10.2307/1941899.

Romme, W. H., M. S. Boyce, R. Gresswell, E. H. Merrill, G. W. Minshall, C. Whitlock, and M. G. Turner (2011), Twenty years after the 1988 Yellowstone fires: Lessons about disturbance and ecosystems, *Ecosystems (N. Y.)*, *14*, 1196–1215, doi:10.1007/s10021-011-9470-6.

Running, S. W. (2008), Climate change: Ecosystem disturbance, carbon, and climate, *Science*, *321*, 652–653, doi:10.1126/science.1159607.

Ryan, C. M., and M. Williams (2011), How does fire intensity and frequency affect miombo woodland tree populations and biomass?, *Ecol. Appl.*, *21*, 48–60, doi:10.1890/09-1489.1.

Ryan, M. G., D. Binkley, and J. H. Fownes (1997), Age-related decline in forest productivity: Pattern and process, *Adv. Ecol. Res*, *27*, 213–262, doi:10.1016/S0065-2504(08)60009-4.

Schimel, D. S., et al. (1997), Continental scale variability in ecosystem processes: Models, data, and the role of disturbance, *Ecol. Monogr.*, *67*, 251–271, doi:10.1890/0012-9615(1997)067[0251:CSVIEP]2.0.CO;2.

Sitch, S., et al. (2008), Evaluation of the terrestrial carbon cycle, future plant geography and climate-carbon cycle feedbacks using five Dynamic Global Vegetation Models (DGVMs), *Global Change Biol.*, *14*, 2015–2039, doi:10.1111/j.1365-2486.2008.01626.x.

Smithwick, E. A. H., M. E. Harmon, and J. B. Domingo (2007), Changing temporal patterns of forest carbon stores and net ecosystem carbon balance: The stand to landscape transformation, *Landscape Ecol.*, *22*, 77–94, doi:10.1007/s10980-006-9006-1.

Smithwick, E. A. H., M. G. Ryan, D. M. Kashian, W. H. Romme, D. B. Tinker, and M. G. Turner (2009), Modeling the effects of fire and climate change on carbon and nitrogen storage in lodgepole pine (*Pinus contorta*) stands, *Global Change Biol.*, *15*, 535–548, doi:10.1111/j.1365-2486.2008.01659.x.

Stinson, G., et al. (2011), An inventory-based analysis of Canada's managed forest carbon dynamics, 1990 to 2008, *Global Change Biol.*, *17*, 2227–2244, doi:10.1111/j.1365-2486.2010.02369.x.

Tilman, D., P. Reich, H. Phillips, M. Menton, A. Patel, E. Vos, D. Peterson, and J. Knops (2000), Fire suppression and ecosystem carbon storage, *Ecology*, *81*, 2680–2685, doi:10.1890/0012-9658(2000)081[2680:FSAECS]2.0.CO;2.

Turetsky, M. R., E. S. Kane, J. W. Harden, R. D. Ottmar, K. L. Manies, E. Hoy, and E. S. Kasischke (2011), Recent acceleration of biomass burning and carbon losses in Alaskan forests and peatlands, *Nat. Geosci.*, *4*, 27–31, doi:10.1038/ngeo1027.

Turner, M. G. (2010), Disturbance and landscape dynamics in a changing world, *Ecology*, *91*, 2833–2849, doi:10.1890/10-0097.1.

Turner, M. G., W. H. Romme, R. H. Gardner, R. V. Oneill, and T. K. Kratz (1993), A revised concept of landscape equilibrium: Disturbance and stability on scaled landscapes, *Landscape Ecol.*, *8*, 213–227, doi:10.1007/BF00125352.

Turner, M. G., W. W. Hargrove, R. H. Gardner, and W. H. Romme (1994), Effects of fire on landscape heterogeneity in Yellowstone National Park, Wyoming, *J. Veg. Sci.*, *5*, 731–742, doi:10.2307/3235886.

Van Wagner, C. E. (1978), Age-class distribution and the forest fire cycle, *Can. J. For. Res.*, *8*, 220–227, doi:10.1139/x78-034.

Vargas, R., M. F. Allen, and E. B. Allen (2008), Biomass and carbon accumulation in a fire chronosequence of a seasonally dry tropical forest, *Global Change Biol.*, *14*, 109–124.

VEMAP Members (1995), Vegetation ecosystem modeling and analysis project - comparing biogeography and biogeochemistry models in a continental-scale study of terrestrial ecosystem responses to climate-change and CO_2 doubling, *Global Biogeochem. Cycles*, *9*(4), 407–437, doi:10.1029/95GB02746.

Webster, P. J., G. J. Holland, J. A. Curry, and H. R. Chang (2005), Changes in tropical cyclone number, duration, and intensity in a warming environment, *Science*, *309*, 1844–1846, doi:10.1126/science.1116448.

Weng, E. S., and Y. Q. Luo (2011), Relative information contributions of model vs. data to short- and long-term forecasts of forest carbon dynamics, *Ecol. Appl.*, *21*, 1490–1505, doi:10.1890/09-1394.1.

Westerling, A. L., M. G. Turner, E. A. H. Smithwick, W. H. Romme, and M. G. Ryan (2011), Continued warming could transform Greater Yellowstone fire regimes by mid-21st century, *Proc. Natl. Acad. Sci. U. S. A.*, *108*, 13,165–13,170, doi:10.1073/pnas.1110199108.